

RSC Advances

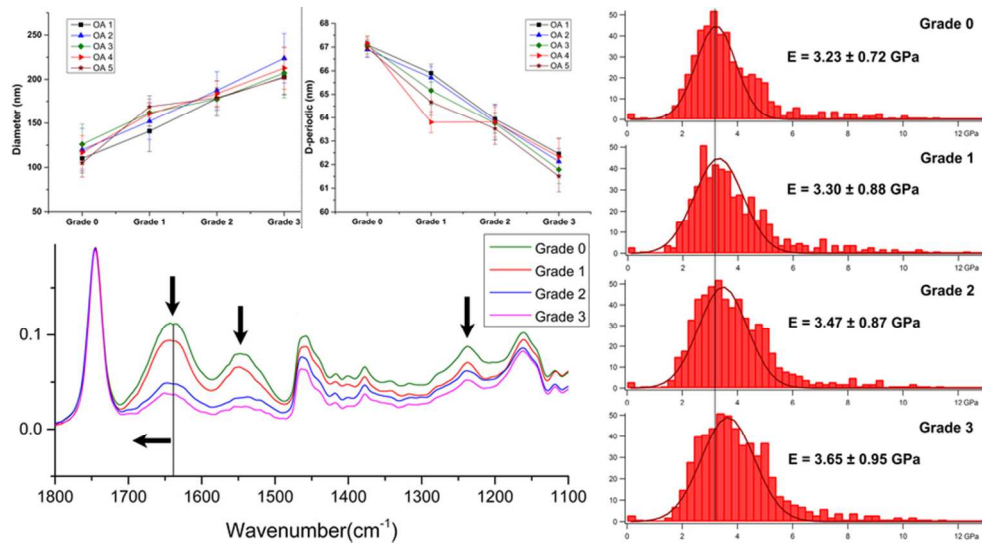


This is an *Accepted Manuscript*, which has been through the Royal Society of Chemistry peer review process and has been accepted for publication.

Accepted Manuscripts are published online shortly after acceptance, before technical editing, formatting and proof reading. Using this free service, authors can make their results available to the community, in citable form, before we publish the edited article. This *Accepted Manuscript* will be replaced by the edited, formatted and paginated article as soon as this is available.

You can find more information about *Accepted Manuscripts* in the [Information for Authors](#).

Please note that technical editing may introduce minor changes to the text and/or graphics, which may alter content. The journal's standard [Terms & Conditions](#) and the [Ethical guidelines](#) still apply. In no event shall the Royal Society of Chemistry be held responsible for any errors or omissions in this *Accepted Manuscript* or any consequences arising from the use of any information it contains.



40x21mm (600 x 600 DPI)

Cite this: DOI: 10.1039/c0xx00000x

www.rsc.org/xxxxxx

ARTICLE TYPE

Structure and nanomechanics of collagen fibrils in articular cartilage at different stages of osteoarthritis

Jundong Shao^{a,b}, Lijun Lin^c, Bin Tang^{*a} and Chang Du^{*b}

Received (in XXX, XXX) Xth XXXXXXXXX 20XX, Accepted Xth XXXXXXXXX 20XX

DOI: 10.1039/b000000x

This study aimed to investigate the variation of structure and nanomechanical properties of human articular cartilage (AC) at different stages of osteoarthritis (OA). The nanoscale morphology, chemical composition, variation of chemical structure, surface adhesion force and elastic modulus were examined. The thickening of collagen fibrils and a decreasing trend of its *D*-periodic banding patterns were observed along with the progression of OA. The calcium and phosphate concentration in AC showed an increasing trend from Grade 0 to Grade 3. These findings suggest that collagen fibrils have reduced intermolecular interactions, greater molecular disorder and decrease in the amount and stability of crosslinks in collagen, which may affect the stability of collagen fibrils. The surface adhesion force showed a decreasing trend while the elastic modulus of individual collagen fibrils showed an increasing trend with the advancement of OA, which was confirmed to have a direct functional consequence in the nanostructure of collagen fibrils. This study is helpful for understanding OA pathogenesis and providing an efficient strategy for pre-symptomatic diagnostics of OA.

Introduction

Osteoarthritis (OA) is the most prevalent type of arthritis and is seen especially among the elderly but people of any age can develop the disease^{1,2}. The most common risk factors for OA include sex, age, obesity, genetics, joint injury and mechanical factors³. The process of OA progression was described microscopically: depletion of proteoglycan (PG), break down of collagen fibrils network, and mechanical failure of articular cartilage (AC), finally worn out⁴. It is generally believed that the cartilage degradation process in OA usually starts with the depletion of PG followed by the degradation of collagen fibrils, which therefore causes the mechanical failure and ultimately complete erosion of the AC⁵. Damage starts at the molecular scale and progressively spreads to the higher structural architecture of AC⁶. However, the underlying molecular processes of OA are poorly understood, making early diagnosis nearly impossible⁷. At present, there are no available treatments so far to attenuate or cure AC degradation in progressive OA until the damaged joint is reconstructed surgically; therefore, it is necessary to detect OA in very early stage when it remains reversible⁸.

With the advent of nanobiotechnology, it will be greatly helpful for the understanding of OA pathogenesis, and might be able to provide an efficient strategy for pre-symptomatic diagnostics of OA^{5,7}. For an instance, atomic force microscope (AFM) is now widely used on imaging and mechanical characterization of biological tissues, due to its ultra high displacement resolution, high sensitivity in force detection and great diversity of applications under various conditions⁹⁻¹¹. Stolz

and colleagues have previously introduced the capability of indentation-type AFM (IT-AFM) for early detection of OA in both animal and human specimens, by imaging the morphology of the AC surface with nanometre resolution and measuring its stiffness at the micrometre and nanometre scales^{12,13}. Moreover, changes in AC due to OA are clearly depicted at the nanometre scale well before microscopical morphological changes can be observed⁵. Stiffening of collagen fibrils meshwork was identified as an early biomarker for the onset of OA^{5,12-14}. The degenerative changes of collagen fibril meshwork in initial stage of OA could be a result of the disruption of individual collagen fibril. Therefore, the change of nanomechanical properties in individual collagen fibrils might be an important indicator for early OA, and thus conducive to understand the onset of OA.

In the previous work of our group, attempts have been made to characterize the *in-situ* nanomechanical behavior of collagen fibrils in the specimens of human articular cartilage with OA^{14,15}. The stiffened collagen fibrils in AC occurred with OA onset and progression. Higher level of fibril calcification in OA affected AC was observed, which might have a higher chance of being broken than healthy fibrils under imposed stress. Then, collagen fibrils were extracted from healthy and OA cartilages by using the extraction buffer to investigate the nanostiffness of individual collagen fibrils¹⁵. The results also demonstrated that the collagen fibrils extracted from OA patients are stiffer than those from healthy patients. Unfortunately, the detailed mechanism for the nanomechanical change of collagen fibrils in OA is still ambiguous.

Herein, we performed an investigation on the variation of structure and nanomechanical properties of human AC at

different stages of OA. Ultrathin frozen tissue section was used to cast two-dimensional (2-D) specimens of human AC at different stages of OA. The micro-scale (bulk AC) and nano-scale (individual collagen fibrils) morphology were observed by using AFM. The variation of composition and chemical structure were characterized using Energy-dispersive X-ray spectroscopy (EDS) and attenuated total reflectance Fourier Transform infrared spectroscopy (ATR-FTIR). Then, individual collagen fibrils were extracted from these 2-D specimens to investigate the nanomechanical properties (surface adhesion force and elastic modulus) by using Force spectroscopy measurement and Nanoindentation based on AFM. A better understanding of structural evolution and nanomechanical properties relationship of AC at different stages of OA will be helpful for pre-symptomatic diagnostics of OA.

Experimental Section

Human Specimens Collection and Preparation

All experimental procedures were approved by the Institutional Review Board of the authors' institute. All these AC specimens with OA were collected from five patients (detail informations of patients were shown in Table S1) undergoing total knee replacement surgery (Southern Medical University, Guangzhou, China), and informed consent document was obtained from every patient. In this study, AC specimens at different stages of OA (labeled as Grade 0-3) were classified by the severity of damage cut from different parts of the same piece of AC. The cutting direction is transverse and the cutting locations are all in the superficial zone of AC. According to the Outerbridge classification system¹⁶, the principal to distinguish each grade is as follow: (1) Grade 0: AC is intact; (2) Grade 1: flaking exists on the superficial of AC; (3) Grade 2: AC suffers from more severe destruction, but no bone is bared; (4) Grade 3: AC suffers from loss of cartilage in one or more loading regions, which damage to deep zone and calcified zone; (5) Grade 4: complete loss of AC occurs with large bone-area exposures.

All these AC specimens were immersed in phosphate buffered saline (PBS) and stored in -24 °C refrigerator before testing. For the preparation of specimens at different stages of OA, the stored specimens were thawed and then cut into small pieces with area around 2 mm² from superficial zone of AC with different stages of OA. The small pieces of AC samples were washed with PBS for 3 times and then covered with tissue freezing medium. After freezing at -24 °C for 30 min, the sample was then sectioned by layers with 5-20 μm in thickness by using a ultrathin frozen tissue section. For AFM imaging, EDS and ATR-FTIR, sections were attached onto the glass slip and washed with PBS for 3 times, then freeze-dried in vacuum lower than 0.5 mmHg for 48 h. For Force spectroscopy measurement and Nanoindentation, sections were also washed with PBS for 3 times and excess liquid was removed with filter paper. The sections were attached onto the anti-off glass slide, covered by a cover slip and applied a small pressure for 30 min. After the section and cover slip were removed, the anti-off glass slide was freeze-dried in vacuum for 48 h, then a small amount of individual collagen fibrils were detached from AC sections.

AFM imaging

The morphology of these sections in both micro-scale (bulk AC) and nano-scale (individual collagen fibrils) were observed employing a MFP-3D-S AFM (Asylum Research, USA) under AC mode (tapping mode) in an air atmosphere. The tip used is a PPP-NCHR probe (Nanosensors) with nominal tip radius less than 7 nm.

EDS and ATR-FTIR

Compositional analysis of full-thickness of a cross section AC with OA was performed at 20 kV using SEM (Quanta 200, FEI, The Netherlands) connected to EDS (INCA 300, Oxford, UK).

ATR-FTIR analysis was performed by a Nicolet, CCR-1 spectrometer at room temperature. A zinc selenide (ZnSe) internal reflection element with a fixed angle of incidence of 45° was used for ATR-FTIR measurements. ATR-FTIR spectra were derived from 64 scans, collected at a resolution of 2 cm⁻¹.

Force spectroscopy measurement and Nanoindentation

Force spectroscopy measurement and Nanoindentation based on AFM were performed under contact mode using Nanosensors PPP-NCHR probe (the tip radius is below 7 nm). The working spring constants were determined with the thermal noise method. The adhesion force between the AFM probe and the surface of individual collagen nanofiber was obtained by force spectroscopy measurement. The nanoindentation test provided the information of deformation behavior and the sample elastic modulus.

Statistical analysis

All data were presented as means ± standard deviation (SD). In order to test the significance of the observed differences between the study groups, analysis of variance (ANOVA) statistical was applied. A value of p < 0.05 was considered to be statistically significant.

Results and Discussion

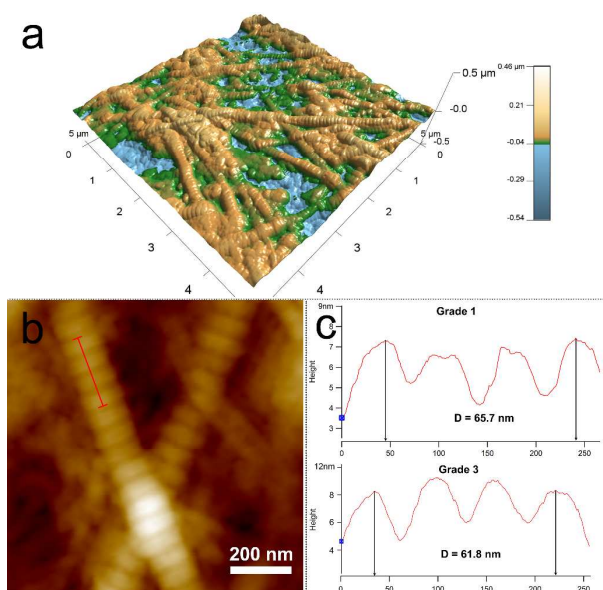


Figure 1: (a) A typical 3D AFM image with range $5 \times 5 \mu\text{m}^2$ of

AC section with OA; (b) a typical AFM image with a higher resolution ($1 \times 1 \mu\text{m}^2$), the red line is the line section analysis; (c) a typical line section analysis result of collagen fibrils from AC section at different stages of OA (Grade 1 and Grade 3).

The AFM imaging experiment studying the surface morphology of the section of AC at different stages of OA was conducted with a PPP-NCHR probe with a tip radius below 7 nm. The excellent tip radius and the minimized variation in tip shape provide more reproducible images and enhanced resolution. AFM imaging was firstly scanned in a larger area on interested location, and then re-scanned with a higher resolution. The images were scanned from the range $20 \times 20 \mu\text{m}^2$ to $0.5 \times 0.5 \mu\text{m}^2$. Then images with range $5 \times 5 \mu\text{m}^2$ were used to analyze the diameter of collagen fibrils, as shown in Figure 1a. AFM images with higher resolution ($1 \times 1 \mu\text{m}^2$) show the detailed structure of collagen fibrils, e.g. the overlap and gap region of the collagen fibrils can be easily identified. *D*-periodic banding pattern of collagen fibrils can be observed in high magnified image (Figure 1b). Statistical measurements on *D*-periodic banding pattern of collagen fibrils were calculated by using line section analysis (Figure 1c).

The statistic of diameter of collagen fibrils ($n=50$) in AC sections at different stages of OA (from Grade 0 to Grade 3) from five different patients (OA 1-5) is shown in Figure 2a. It's clearly that the average diameters of collagen fibrils in AC specimens showed a gradual thickening trend during OA progression, which is in agreement with our previous finding using SEM¹⁴. Figure 2b shows the statistical measurement of the corresponding *D*-periodic banding pattern of collagen fibrils. Each data point is the average of several *D*-periodic banding patterns of single collagen fibril as shown in Figure 1c. Alteration of *D*-periodic banding patterns of collagen fibrils was observed and showed a decreasing trend from 67 nm to about 62 nm with the progression of OA. Figure 1c shows the image analysis result of two collagen fibrils from Grade 1 and Grade 3 respectively. The width of *D*-periodic banding pattern exhibited apparent decrease during OA progression.

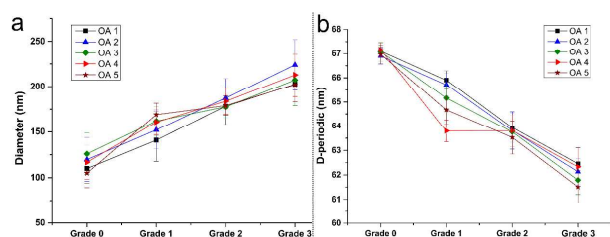


Figure 2: (a) The average diameters of collagen fibrils with standard deviation ($n=50$) from AC sections at different stages of OA (Grade 0-3) from different patients (OA 1-5); (b) the corresponding *D*-periodic banding pattern ($n=20$). Except the Grade 1 and 2 from OA4 in Figure 2b, all groups of data showed statistically significant difference ($p < 0.05$, ANOVA).

At the lowest hierarchical level of structure, collagen fibrils are composed of collagen molecules with three peptide chains. It forms with an order of 67 nm *D*-periodic structure in respect to the adjacent molecule to synthesize the collagen fibrils¹⁷. Therefore, the increase in diameter and the decrease in *D*-periodic banding pattern of collagen fibrils observed indicates that the composition and molecular structure of individual collagen fibrils

in AC might change during OA progression. The structure change of collagen fibrils would cause the mechanical failure of collagen meshwork, which results in the degradation of AC, the major reason for OA progression.

To further investigate the variation of structure of collagen fibrils from these AC sections at different stages of OA, Energy-dispersive X-ray spectroscopy (EDS) and attenuated total reflectance Fourier Transform infrared spectroscopy (ATR-FTIR) were used for the composition analysis and the characterization of the variation of chain conformation.

For the EDS measurement, a cross section of AC specimens was used, which contains parts of AC with Grade 0-3 OA. After imaged by SEM, EDS was performed to scan the calcium (Ca) and phosphate (P) in the selected area (Figure S1). The Ca or P content was expressed as the distribution density of the element on the area analysis patterns of the AC sections by EDS, and Figure 3 shows the typical results. A gradual increase of Ca and P concentration can be clearly observed from Grade 0 to Grade 3. Although the content of Ca and P in the total composition is very low (below 2%), calcium/phosphate deposition might be associated with the nanomechanical properties of collagen fibrils in OA cartilage¹⁴.

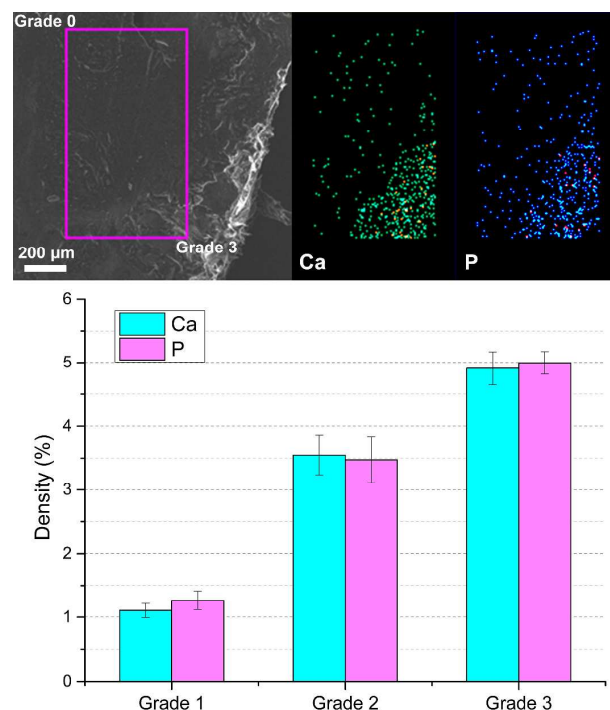


Figure 3: Typical EDS results and the distribution density of Ca and P element on the area analysis patterns of the AC sections by EDS.

ATR-FTIR was used for the further characterization of AC sections at different stages of OA due to its distinct IR absorption patterns of AC with different chemical structure in characteristic bands. FTIR has been used previously to study changes in the secondary structure of collagen. Many vibrational bands characteristic of peptide groups and side chains provide information on protein structures^{18,19}, such as changes in the amide I ($1636\text{-}1661 \text{ cm}^{-1}$), amide II ($1549\text{-}1558 \text{ cm}^{-1}$) and the

amide III (1200-1300 cm^{-1}) regions. Figure 4 shows typical FTIR spectra in the the range 3750-550 cm^{-1} of various AC sections at different stages of OA. All the spectra were overlapped and normalized according to the peak at about 1749 cm^{-1} attribute to the carbonyl stretching vibration [$\nu(\text{C}=\text{O})$] and the inset graph is the enlarged spectral region of 1800-1100 cm^{-1} .

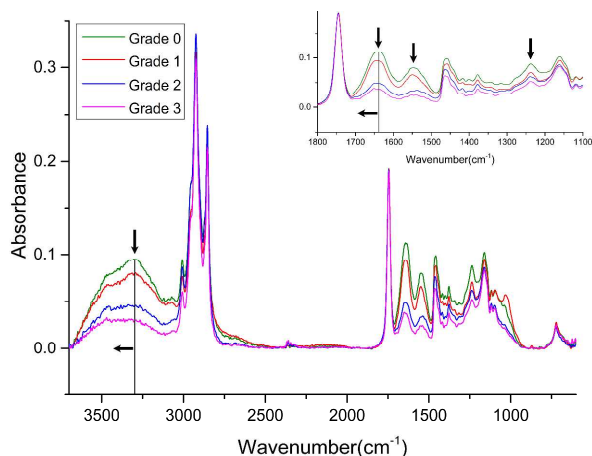


Figure 4: Typical ATR-FTIR spectra in the range 3750-550 cm^{-1} of various AC sections at different stages of OA. The inset graph is the enlarged spectral region of 1800-1100 cm^{-1} .

All these AC sections display bands at about 1640 cm^{-1} , 1550 cm^{-1} and 1240 cm^{-1} , which are characteristic of the amide I, II and III bands of collagen²⁰. As shown in Figure 4, reduction in the intensity of amide I, II and III peaks and a slight shift to higher wave number of amide I peak can be observed clearly. These features are associated with reduced intermolecular interactions in collagen¹⁸. On the other hand, the amide A band arising from N-H stretching, which is located at about 3310 cm^{-1} , also showed a decreasing trend in the intensity and shift to higher wave number. The triple helices of collagen are mainly held together by hydrogen bonds and the amide A band is associated directly with the triple-helical conformation²¹. These changes are indicative of greater molecular disorder and decrease in the amount and stability of crosslinks¹⁸ in collagen from the AC section with later stage of OA, which will affect the stability of collagen fibrils. This result further confirmed that the breakdown of collagen molecules in OA is accompanied by changes in fibril alignment²².

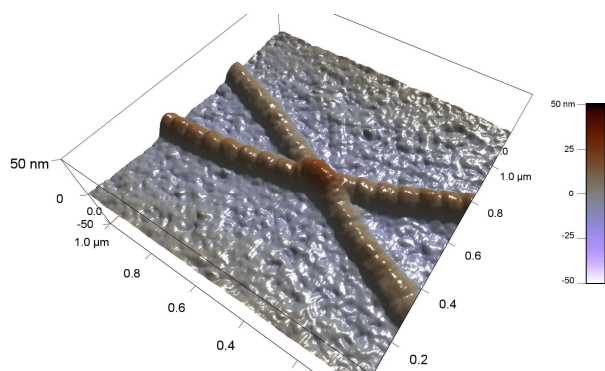


Figure 5: A typical 3D AFM image of individual collagen fibrils extracted from AC section by using an anti-off glass slide.

Then, Force spectroscopy measurement and Nanoindentation based on AFM were used to investigate the nanomechanical

properties (adhesion force and elastic modulus) of individual collagen fibrils extracted from AC sections at different stages of OA (Figure S2). These measurements were performed under contact mode using PPP-NCHR probe and the cantilever spring constants were calibrated to be 20.36 nN/nm using the thermal noise method. Figure 5 shows a typical 3D AFM image of individual collagen fibrils extracted from AC sections at different stages of OA by using an anti-off glass slide.

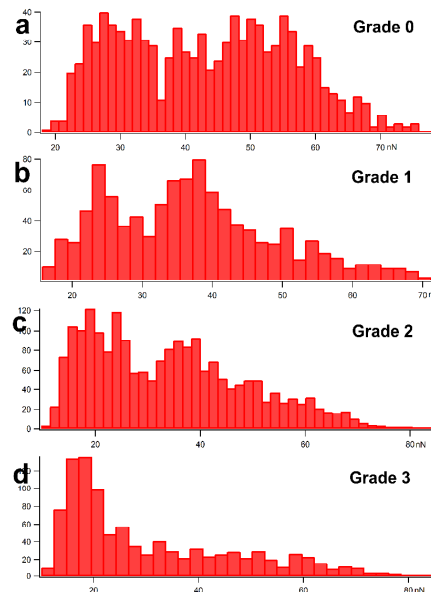


Figure 6: The frequency histograms of F_{ad} for AC specimens at different stages of OA.

The adhesion force (F_{ad}) between the probe and the surface of collagen fibril was obtained by Force spectroscopy measurement under contact mode and the value was determined using Igor Pro 6.21A software. F_{ad} takes retract force and takes the difference between the minimum value and the average of the last 5 points. Basically, the F_{ad} obtained in the air is the superposition of electrostatic, van der Waals, and capillary and interfacial tension forces. In this study, since the samples were freeze-dried in vacuum and the tests were performed under an air humidity less than 30%, the contributions of capillary and superficial tension forces were minimized and the van der Waals and solid-solid interfacial forces can be regarded as major contributors to the F_{ad} ²³. A force-map (32 points over 32 lines) was recorded over a $1 \times 1 \mu\text{m}^2$ area of interest. The probe position was raster scanned over the sample surface after each force plot. Force-distance curves collected at each probe position were digitally stored for subsequent analysis and the value of adhesion force can be determined using MFP-3D software. About 1000 individual force spectra from 10 force-maps corresponding to the collagen fibril were extracted to produce a probability histogram of F_{ad} .

As shown in Figure 6, the distribution of F_{ad} values for different AC specimens varies significantly. For the Grade 0 specimen, F_{ad} values were uniformly distributed in the range from 22 nN to 60 nN . For the Grade 1 specimen, F_{ad} values were mainly distributed in the range from 18 nN to 50 nN with two peaks at about 24 nN and 38 nN . While for the Grade 2 specimen, this range is reduced to 15-50 nN , also with two peaks at about 20 nN and 35 nN . With same trend, F_{ad} values for the Grade 3 specimen decreased to the range 10-25 nN with a peak at about 17 nN . Apparently, the F_{ad} between the probe and the surface of

collagen fibrils show a decreasing trend with the development of OA. In our previous work, the nanostructure of polymer nanofiber was confirmed to have a direct functional consequence in the nanoscale mechanical property²⁴⁻²⁶. This result clearly demonstrates that the nanostructure of collagen fibril changed to have a greater molecular disorder arrangement occurred with OA onset and progression.

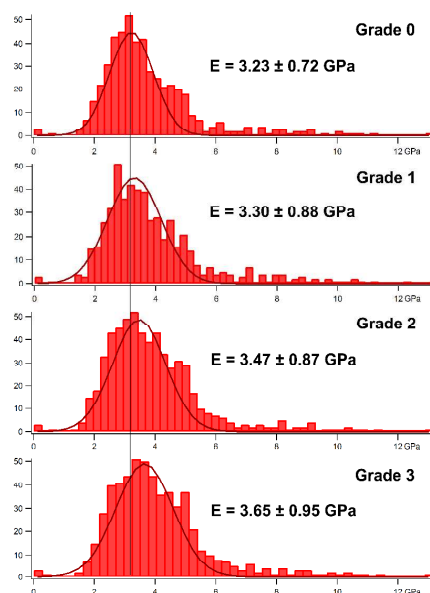


Figure 7: The frequency histograms of E_{sam} for AC specimens at different stages of OA. The histogram was fitted by the Gaussian curve and the average values were expressed as mean \pm width. All groups of data showed statistically significant difference ($p < 0.05$, ANOVA).

The nanoindentation test provides information of deformation behaviour and the sample modulus. The data were fitted with the Hertzian model²⁷ and the value of the sample modulus can be determined using Igor Pro 6.21A software^{25,26}. All the force curves were taken on the central part of the collagen fibril to avoid geometric effects. The frequency histograms of elastic modulus (E_{sam}) were shown in Figure 7. The data was collected from nanoindentation test on several collagen fibrils with the total indentation points over 500. The histogram was fitted by the Gaussian curve and the position of the maximum of the Gaussian component was taken as the most probable E_{sam} .

It was found that the E_{sam} of collagen fibrils showed a slight increasing trend with OA initiation and progression (Grade 0 to 3). The trend of individual collagen fibril stiffening did not change with the breakdown of collagen meshwork with advancement of OA. This result could be also one of possible reasons for increased stiffness of collagen fibrils meshwork in the initial stage of OA¹⁴. The increase of the E_{sam} of collagen fibrils with advancement of OA might be associated with both the calcium/phosphate deposition and the nanostructure variation.

Conclusions

In summary, the variation of structure and nanomechanical properties of human AC at different stages of OA were systematically investigated. A gradual thickening trend of collagen fibrils and a decreasing trend of D -periodic banding pattern were observed during OA progression. A gradual increase of Ca and P concentration can be clearly observed in SEM-EDS

from Grade 0 to Grade 3. Greater molecular disorder and decrease in the amount and stability of crosslinks were confirmed by ATR-FTIR, which will affect the stability of collagen fibrils. A decreasing trend in F_{ad} further confirmed that collagen fibrils have a greater molecular disorder arrangement occurred with OA onset and progression. The elastic modulus of individual collagen fibril increases with the advancement of OA. It is believed that this study should lead to a better understanding of OA pathogenesis and provide an efficient strategy for pre-symptomatic diagnostics of OA.

Acknowledgements

The work was financially supported by National Basic Research Program of China (2012CB619100), the National Natural Science Foundation of China (50830101, 51072056), Key grant of Chinese Ministry of Education (313022), Program for New Century Excellent Talents in University (NCET-08-0210), Program for Changjiang Scholars and Innovative Research Team in University (IRT 0919), NSFC project grant 11202039 and basic research grant from ShenZhen Government (No.201208303000415).

Notes and references

- ^a Department of Materials Science and Engineering, South University of Science and Technology of China, Shenzhen 518055, PR China. Email: tangbinsci@gmail.com; Tel: 86-0755-88018998
- ^b School of Materials Science and Engineering, South China University of Technology, Guangzhou 510641, PR China. E-mail: duchang@scut.edu.cn; Tel: 86-020-22236062
- ^c Department of Orthopedics, Zhujiang Hospital, Southern Medical University, Guangzhou, Guangdong, China
- U. Styrkarsdottir, G. Thorleifsson, H. T. Helgadóttir, et al. *Nature Genetics*, 2014, 46, 498-502.
- R. F. Loeser, S. R. Goldring, C. R. Scanzello, et al. *Arthritis & Rheumatism*, 2012, 64, 1697-1707.
- M. Blagojevic, C. Jinks, A. Jeffery, K. P. Jordan, *Osteoarthritis Cartilage*, 2010, 18, 24-33.
- J. Martel-Pelletier, D. Lajeunesse, H. Fahmi, et al. *Current rheumatology reports*, 2006, 8, 30-36.
- M. Stolz, R. Gottardi, R. Raiteri, et al. *Nature Nanotechnology*, 2009, 4, 186-192.
- H. A. Wieland, M. Michaelis, B. J. Kirschbaum and K. A. Rudolph, *Nature reviews Drug discovery*, 2005, 4, 331-344.
- T. Aigner, N. Schmitz, J. Haag, *Nature nanotechnology*, 2009, 4, 144-145.
- T. C. B. Pollard, S. E. Gwilym, A. J. Carr, *Journal of Bone & Joint Surgery, British Volume*, 2008, 90, 411-421.
- C. T. McKee, J. A. Last, P. Russell, et al. *Tissue Engineering Part B: Reviews*, 2011, 17, 155-164.
- N. E. Kurland, Z. Drira, V. K. Yadavalli, *Micron*, 2012, 43, 116-128.
- E. K. Dimitriadis, F. Horkay, J. Maresca, et al. *Biophysical journal*, 2002, 82, 2798-2810.
- M. Stolz, R. Raiteri, A. U. Daniels, et al. *Biophysical Journal*, 2004, 86, 3269-3283.
- M. Stolz M, U. Aebi, D. Stoffler, *Nanomedicine: Nanotechnology, Biology and Medicine*, 2007, 3, 53-62.
- C. Y. Wen, C. B. Wu, B. Tang, et al. *Osteoarthritis and Cartilage*, 2012, 20, 916-922.
- B. Tang, M. K. Fong, C. Y. Wen, et al. *Soft Materials*, 2014, 12, 253-261.
- R. E. Outerbridge, J. A. Dunlop, *Clinical Orthopaedics and Related Research*, 1975, 110, 177-196.
- O. Antipova and J. P. R. O. Orgel, *Journal of Biological Chemistry*, 2010, 285, 7087-7096.

-
- 18 J. H. Muyonga, C. G. B. Cole, K. G. Duodu, *Food Chemistry*, 2004, 86, 325-332.
- 19 E. P. Paschalis, K. Verdelis, S. B. Doty, et al. *Journal of bone and mineral research*, 2001, 16, 1821-1828.
- 5 20 A. Sionkowska, M. Wisniewski, J. Skopinska, et al. *Biomaterials*, 2004, 25, 795-801.
- 21 M. C. Chang, J. Tanaka, *Biomaterials*, 2002, 23, 4811-4818.
- 22 H. E. Panula, M. M. Hyttinen, J. P. A. Arokoski, et al. *Annals of the Rheumatic Diseases*, 1998, 57, 237-245.
- 10 23 L. Sirghi, M. Nakamura, Y. Hatanaka, et al. *Langmuir*, 2001, 17, 8199-8203.
- 24 J. Shao, C. Chen, Y. Wang, et al. *Reactive and Functional Polymers*, 2012, 72, 765-772.
- 25 J. Shao, C. Chen, Y. Wang, et al. *Applied Surface Science*, 2012, 258, 6665-6671.
- 15 26 J. Shao, Y. Wang, X. Chen, et al. *Colloids and Surface B: Biointerfaces*, 2014, 120, 97-101.
- 27 K. B. Crozier, G. G. Yaralioglu, F. L. Degertekin, et al. *Applied Physics Letters*, 2000, 76, 1950-1952.